Highlight Review

Ligand Influences in Heme–Copper O_2-Chemistry as Synthetic Models for Cytochrome *c* Oxidase

Kenneth D. Karlin* and Eunsuk Kim

(Received May 31, 2004; CL-048008)

Abstract

Prominent recent advances in synthetic modeling chemistry of cytochrome *c* oxidase include the generation and characterization of high-spin heme–peroxo–copper species derived from $Fe^{II}/Cu^{I}/O_2$ reactions. Comparison of spectroscopic properties of a series of related complexes leads to a finding that the coordination nature of the peroxo bridging group binding between heme and copper can be dramatically altered by copper ligand environment. Intrinsic copper/O_2 interactions seem to be applicable to the chemistry of heme/Cu/O_2 systems.

♦ Introduction

The cytochrome *c* oxidase (C*c*O) heme–copper active site structure, physical properties, and reaction chemistry continues to intrigue biochemists, biophysicists, and inorganic chemists. For synthetic bioinorganic chemists, the metal center that has attracted the most attention is the heme–copper binuclear site, where a heme and proximal (≈4.4–5.3 Å, see below) copper ion center effects O_2-binding and O–O reductive cleavage.[1] In this article, we overview efforts to mimic or 'model' aspects of the dioxygen reactivity in heme plus copper environment, focusing on the considerable recent advances, including our own work which reveals the strong influence of the nature of the copper ligand upon the structure and spectroscopic properties of heme–O_2–copper adducts.

The chemistry at metalloprotein active sites cannot be disconnected from the metal's inherent fundamental chemistry, thus the study of well-defined small-molecule active-site synthetic models can provide great insight.[2] The purpose of models is not necessarily to exactly duplicate biological structural or reactivity traits. Rather, biomimetic chemistry serves to sharpen or focus relevant questions, in part through the determination of fundamental aspects of structure, spectroscopy, magnetic, and electronic structure, as well as reactivity and chemical mechanism. The synthetic analog approach can be used to investigate the effects of systematic variations in coordination number and geometry, donor atom type, local environment, and other factors, often providing insights that cannot be easily deduced from protein studies. Heme–O_2[3,4] and copper–dioxygen[5–8] chemistries are separately well studied, however the reactivity of O_2 in a heme/copper environment is less well established.[1] Desirable fundamental advances are in the areas of dynamics of heme/Cu/O_2 reactions, structure of products and their associated spectroscopy, and O_2-reduction & O–O cleavage chemistry.

C*c*O is a terminal respiratory membrane-bound protein composed of up to 13 subunits (in the bovine enzyme). It catalyses the four-electron, four-proton reduction of dioxygen to water, coupling this reaction to the generation of a *trans*-membrane proton gradient, by effecting the translocation ('pumping') of four protons per O_2 molecule reduced.

$$O_2 + 4\ e^- + 8\ H^+_{in} \rightarrow 2\ H_2O + 4\ H^+_{out}$$

The electrochemical potential gradient thus generated provides the driving force needed by ATP synthase, completing the transduction of energy available in the O_2-to-water reduction to provide our chemical energy source (i.e., ATP).[1,9,10]

The primary enzyme activity resides in enzyme subunits I and II. Soluble cytochrome *c* docks and transfers reducing equivalents one-at-a-time to the novel dicopper (Cu_A) electron-transfer center, a binuclear cysteine-bridged (i.e., His–Cu–(μ-Cys)$_2$–Cu–His) mixed-valence (Cu(1.5)–Cu(1.5)) site. Electrons are subsequently passed on to low-spin heme-*a* and then on to the key binuclear heme-a_3/Cu_B center (Figure 1). The heme-a_3 structure is similar to that of hemoglobin or myoglobin, a high-spin center with proximal histidine. Cu_B is located on the distal side and itself possesses three–histidine–imidazole ligands, one of which is covalently crosslinked to a tyrosine derived phenol. This detailed structural information derives from X-ray structures[11–15] on a number of heme–copper oxidase derivatives (initially coming in 1995 from Yoshikawa[16] in Japan and Michel[17] in Germany). Reduced enzymes have $Fe^{II}\cdots Cu^{I}$ distances of 5.2 Å (Figure 1),[11,18] while various oxidized derivatives possess $Fe^{III}\cdots Cu^{II}$ separations varying from 4.4 to 5.3 Å.[1] The longtime dogma in the field has been that a bridging ligand (such as hydroxide) mediates strong $Fe^{III}\cdots Cu^{II}$ antiferromagnetic coupling. However, the Fe···Cu distances would seem to preclude such an interaction; Thomson and co-workers recently showed that in fact the interaction is very weak ($|J| \approx 1\ cm^{-1}$).[19]

Based on extensive kinetic-spectroscopic investigations, there is now agreement on many aspects of the O_2-binding and reduction process at the heme–copper active site (Figure 1).[1]

Prof. Kenneth D. Karlin
Department of Chemistry, Johns Hopkins University,
Remsen Hall/ 3400 North Charles St., Baltimore, MD 21218-2685, U.S.A.
E-mail: karlin@jhu.edu
Dr. Eunsuk Kim
Department of Chemistry, Johns Hopkins University,
Remsen Hall/ 3400 North Charles St., Baltimore, MD 21218-2685, U.S.A.
E-mail: ekim4@jhu.edu

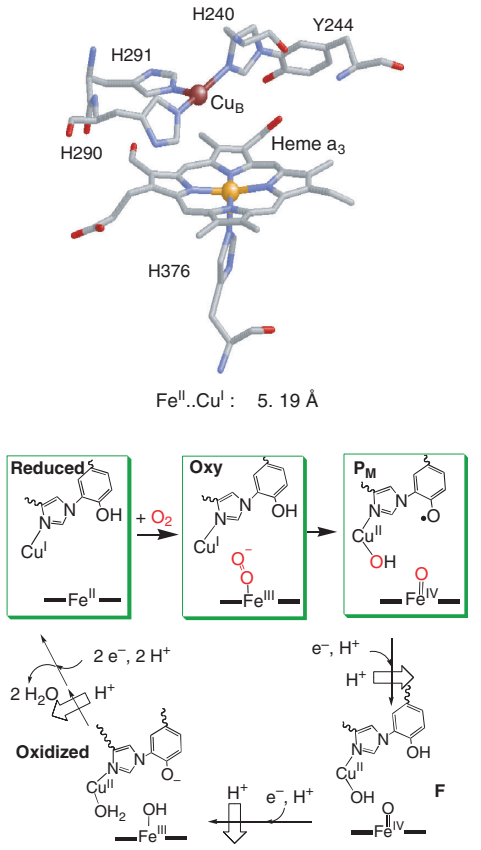

Figure 1. Heme–Cu active site of reduced bovine C*c*O, and indication of the O_2-binding and reductive cleavage mechanism. See text.

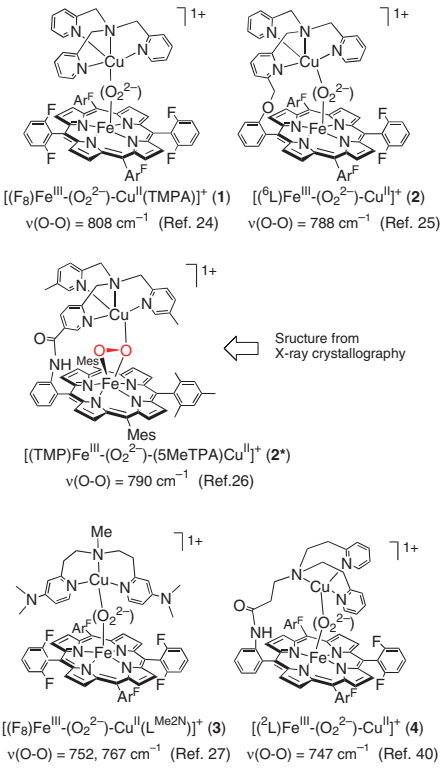

Figure 2. Dioxygen adducts derived from heme–copper reduced precursor complexes. All are peroxo-bridged high-spin antiferromagnetically coupled (S = 2) heme-Fe^{III}–(O_2^{2-})–Cu^{II} species, which have been characterized by a variety of physical-spectroscopic techniques, including resonance Raman spectroscopy, for which results are provided.

Cu_B appears to initially bind dioxygen, thus highlighting the importance of insights into fundamental aspects of Cu^I/O_2 reactivity. In fact, recent work from the authors' laboratories show that a copper(I) complex is capable of binding O_2 at near diffusion controlled rates.[20] The O_2-ligand then transfers (at an overall rate of $\approx 10^5\ s^{-1}$) to heme-a_3 iron forming an initial 'Oxy' Fe–O_2 adduct (Figure 1) which is structurally and spectroscopically analogous to oxy-hemoglobin/myoglobin.

In the next observable intermediate, the O–O bond has been reductively cleaved; but the detailed nature of the active site products depends on whether one starts the experiments with fully reduced enzyme or in the 'mixed-valent' form (with only heme–Cu binuclear center reduced).

Ferryl Fe^{IV}=O and Cu^{II}–X (X = OH^- or H_2O) products are generated in '$\mathbf{P_M}$'. The source of the fourth electron is not confirmed; the tyrosine from the His–Tyr 'cofactor' is one possibility (as a proton *and* electron source, as shown in Figure 1), but oxidation of a nearby tryptophan has been alternatively suggested.[1,21] Reduction and protonation lead to intermediate '**F**' (Figure 1), and the resting oxidized state is regenerated after the fourth electron-transfer and protonation to give water. Proton pumping (for which discussion is not included here) accompanies formation of the late intermediates (Figure 1).

♦ *Heme/Cu/O_2 Complexes For Comparison and Contrast*

As outlined in the Introduction, a major goal has been to provide new insights into heme/copper dioxygen reactivity. The groups of Collman,[3,22] in particular, as well as Boitrel,[23] have carried out extensive electrocatalytic O_2-reduction chemistry studies with heme–copper assemblies. These efforts show that C*c*O model compounds can efficiently effect the four-electron four-proton O_2-reduction process and these studies provide insights into the factors which optimize such electrode surface chemistry; recent reviews are available.[3,22]

Here, we emphasize the generation and characterization of discrete O_2-derived complexes, with a series of complexes possessing pyridyl/alkylamine chelates for copper, in association with tetraarylporphyrinates. A recent computational study[21] of the O–O cleavage process in C*c*O utilizes as a starting point a bridged peroxo heme–copper species, that possibly generated after the 'Oxy' intermediate (Figure 1) forms. While the Fe···Cu distances in heme–copper oxidases seems to preclude formation of a discreet Fe–O–O–Cu species (having reasonable metal–O and O–O bonding distances),[1] there is a need to study dioxygen binding and reactivity within heme–copper assemblies, since subsequent O–O reductive cleavage leads to intermediates such as $\mathbf{P_M}$ and **F** (Figure 1), where O atoms derived from O_2 eventually ligate to the heme and copper.

Complexes **1**–**4** (Figure 2) are peroxo-bridged heme–Fe^{III}/Cu^{II} assemblies,[24–28] containing either tetradentate or tridentate chelates for copper. For **1** and **3**, the assemblies are derived from 1:1 mixtures of heme–iron(II) and copper(I) complexes in reactions with dioxygen, while for **2**, **2***, and **4**, more involved syntheses provide for preformed heterobinuclear heme–Fe^{II}/Cu^{I}

Published on the web (Advance View) August 28, 2004; DOI 10.1246/cl.2004.1226

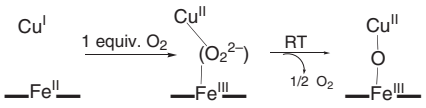

Scheme 1.

complexes which react with O_2 to form related products. Figure 2 also includes vibrational data related to the O–O stretching frequency of the peroxo moiety in these complexes. It is the large variation observed as a function of complex and identity of the copper chelate, from 808 cm^{-1} in **1** to a much reduced value of 747 cm^{-1} in **4**, which is one of the primary topics for discussion in this article.

In all cases, a similar chemistry occurs with these ligand/metal-complex systems (Scheme 1). Reduced complexes, either discrete binuclear compounds or 1:1 mixtures of heme and copper complexes, react with O_2 to form μ-peroxo heme–Cu assemblies. These transform by disproportionation to μ-oxo heme–copper complexes.

♦ *Heme/Cu/O_2 Complexes with Tetradentate Copper Ligands*

In our initial studies, we chose to use TMPA [≡ tris(2-pyridylmethyl)amine] as the copper-chelate, since its O_2-reactivity with $[(TMPA)Cu^{I}(RCN)]^{+}$ was already well established in our group.[29,30] It initially forms an adduct, a superoxocopper(II) species $[(TMPA)Cu^{II}(O_2^{-})]^{+}$,[20,29,30] with as yet unknown structure (i.e., end-on or side-on bound O_2^{-} ligand ?), but reacts further with a second equiv. of reduced copper complex to form the μ-1,2-peroxodicopper complex $[\{(TMPA)Cu^{II}\}_2(O_2^{2-})]^{2+}$ ($\lambda_{max} = 525$ nm, Cu···Cu = 4.38 Å, $\nu_{O-O} = 832\ cm^{-1}$). But, when a 1:1 mixture of $(F_8)Fe^{II}$ and $[(TMPA)Cu^{I}(RCN)]^{+}$ are reacted with dioxygen (one equiv.; spectrophotometric O_2-titration), the heterobinuclear μ-peroxo complex $[(F_8)Fe^{III}–(O_2^{2-})–Cu^{II}(TMPA)]^{+}$ (**1**) (Figures 2 and 3) is generated; no homonuclear peroxo products such as $[\{(TMPA)Cu^{II}\}_2(O_2^{2-})]^{2+}$ or $[(F_8)Fe^{III}–(O_2^{2-})–Fe^{III}(F_8)]$ are formed. Complex **1** thermally converts into μ-oxo complex $[(F_8)Fe^{III}–(O^{2-})–Cu^{II}(TMPA)]^{+}$ (Figure 5); the oxo atom is derived from O_2, as judged by a new isotope sensitive IR band at 856 cm^{-1}. The peroxo-to-oxo complex transformation involves evolution of 0.5 equiv. of dioxygen, indicative of a peroxide disproportionation reaction.[24]

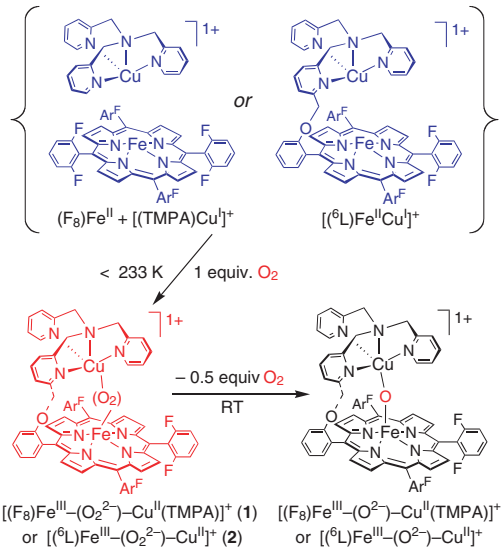

Figure 3. Chemistry of heme–copper complexes employing the TMPA tetradentate tripodal ligand for copper. Either from 1:1 mixtures of heme and copper components or with the binucleating ligand ^{6}L, reduced Fe^{II}–Cu^{I} complexes react with O_2 forming μ-peroxo Fe^{III}–(O_2^{2-})–Cu^{II} complexes. These are stable if kept cold, but transform thermally to μ-oxo complexes.

The chemistry of the $(F_8)Fe^{II}/[(TMPA)Cu^{I}(RCN)]^{+}/O_2$ reaction can be followed by various means, including UV–vis and NMR spectroscopies.[24] The ^{1}H NMR spectrum of $[(F_8\text{-}d_8)Fe^{III}–(O_2^{2-})–Cu^{II}(TMPA)]^{+}$ (**1**) shows a single broad downfield paramagnetically shifted resonance at δ 68 (−40 °C). Upfield shifted resonances assignable to the Cu–TMPA ligand hydrogens in **1** are consistent with an overall $S = 2$ formulation, arising from strong antiferromagnetic coupling of high-spin iron(III) and copper(II) ions.[31] Transformation of **1** to μ-oxo complex $[(F_8)Fe^{III}–(O^{2-})–Cu^{II}(TMPA)]^{+}$ (δ 82 and also upfield Cu-ligand resonances) shows the latter to be a distinctively different compound, but also an $S = 2$ system.[32]

Binucleating ligand ^{6}L can be generated by standard procedures, and metallation leads to the 'empty tether' high-spin hydroxy-iron(III) complex $(^6L)Fe^{III}$–OH, Scheme 2.[25,33,34] Reduction affords $(^6L)Fe^{II}$ where NMR spectroscopic evidence (in toluene or CH_2Cl_2 solvents) suggests that one pyridine coordinates, giving a five-coordinate high-spin complex, as shown. Coordinating solvents (e.g., THF, MeCN or acetone) compete with the pyridine and five or six-coordinate solvento iron(II) species instead form. Addition of a copper(I) salt affords $[(^6L)Fe^{II}Cu^{I}]^{+}$, Scheme 2. This undergoes essentially the same chemistry as observed for the component mixture described above, Figure 3. The μ-peroxo complex $[(^6L)Fe^{III}–(O_2^{2-})–Cu^{II}]^{+}$ (**2**) possesses, as noted (Figure 2) a ν(O–O) stretching frequency which is 20 cm^{-1} lower than that observed for $[(F_8)Fe^{III}–(O_2^{2-})–Cu^{II}(TMPA)]^{+}$ (**1**).

This presumably derives from a change in peroxo structure/binding caused by ligand constraints in the ^{6}L system. Such ligand induced influences are in fact observed when comparing the X-ray structure and other properties (e.g., oxo ligand basicity) of the corresponding μ-oxo complexes, $[(F_8)Fe^{III}–(O^{2-})–Cu^{II}(TMPA)]^{+}$ vs $[(^6L)Fe^{III}–(O^{2-})–Cu^{II}]^{+}$.[34]

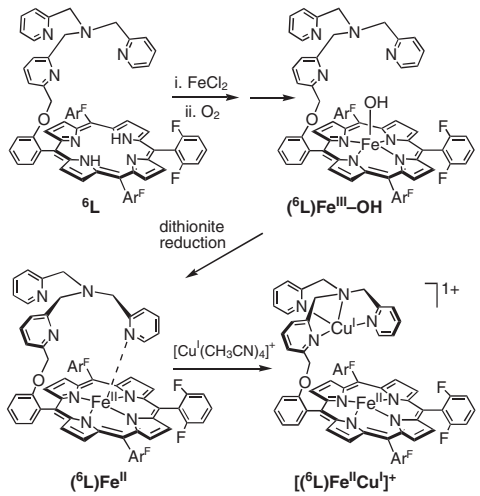

Scheme 2. Synthetic chemistry of ^{6}L containing iron and iron–copper complexes.

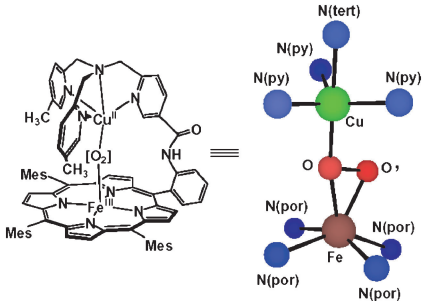

Figure 4. Representation of the heme–peroxo–copper complex from Naruta and co-workers, including the X-ray structure. See text for further description.

♦ *X-ray Structure of a Heme-Peroxo-Copper Complex*

Naruta and co-workers have also been studying heme–copper/dioxygen chemistry with similar kinds of ligand systems.[1,26,35] A remarkable achievement and important advance is the recent X-ray structural characterization of $[(TMP)Fe^{III}–(O_2^{2-})–(5MeTPA)Cu^{II}]^+$ (**2***) (Figures 4 and 2), formed by O_2-reaction with reduced complex $[(TMP)Fe^{II}–(5MeTPA)-Cu^{I}]^+$.[26] A key to the thermal stabilization and crystallization was seen to be the employment of the porphyrin mesityl *meso* groups and methyl substituents on the TMPA ligand. Detailed characterization shows the complex to also (like **1** and **2**, Figure 2) be a high-spin iron(III) $S = 2$ system. (Mössbauer spectroscopy: $\Delta E_Q = 1.17\,mm/s$, $\delta = 0.56\,mm/s$). The O–O stretching frequency is $790\,cm^{-1}$ ($\Delta^{18}O_2 = -44\,cm^{-1}$), in the same range as the other complexes discussed (**1** and **2**), with tetradentate TMPA derived ligand for copper.

The X-ray structure of **2*** shows that the bridging peroxide ligand is coordinated to the iron(III) and copper(II) ions in an asymmetric μ-η^2:η^1 fashion.[26] Here, both oxygen atoms are ligated to the iron (Fe–O = 1.89 Å, Fe···O′ = 2.03 Å) whereas only one oxygen atom is bound to Cu, Cu–O = 1.92 Å, Cu···O′ = 2.66 Å. The O–O bond length is 1.46 Å, exactly in the range expected for a peroxide O–O bond distance. The iron atom is 0.595(10) Å out of the porphyrin plane towards the peroxide ligand, as expected for a high-spin system. The ∠Fe–O–Cu bond angle is 166.0(3)°, similar to that of a related μ-oxo complex $[(^6L)Fe^{III}–(O^{2-})–Cu^{II}]^+$ [∠Fe–O–Cu = 171.1(3)°], whereas the structure of the Cu–O–O unit in **2*** is similar to that of $[\{(TMPA)Cu^{II}\}_2(O_2^{2-})]^{2+}$ (see below), with trigonal bipyramidal copper(II) geometry with peroxo O-atom in an axial position. The similarity of the binucleating ligand structure in **2***, with that present in $[(F_8)Fe^{III}–(O_2^{2-})–Cu^{II}(TMPA)]^+$ (**1**) and $[(^6L)Fe^{III}–(O_2^{2-})–Cu^{II}]^+$ (**2**), along with the observed similar O–O stretching frequencies (all in the range ν(O–O) = 788 to $808\,cm^{-1}$, Figure 2), makes it a reasonable hypothesis that μ-η^2:η^1 peroxo-binding is present in all of these complexes.

♦ *Heme/Cu/O_2 Complexes with Tridentate Copper Ligands*

As part of a systematic approach to elucidating fundamental aspects of heme–copper/dioxygen chemistry, we have wanted to vary the ligand environment, especially around the copper ion. This is because it is well known in copper(I)–dioxygen chemistry that the denticity dramatically alters the nature of the product

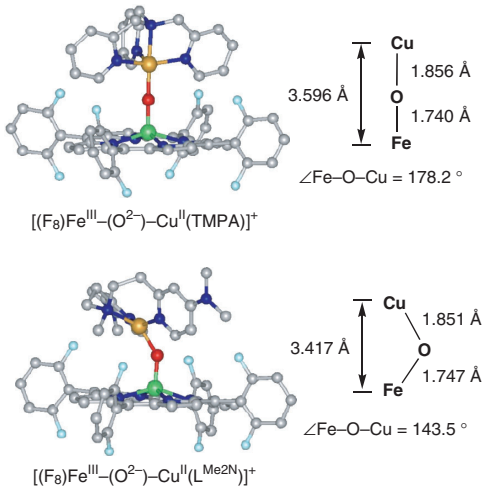

Figure 5. X-ray structural representations of μ-oxo heme–Cu assemblies, revealing the dramatic structural variations in the Fe^{III}–O–Cu^{II} core angle, when the copper possesses a tetradentate (TMPA) versus tridentate (L^{Me2N}) chelate.

formed.[5–8] With this background, we therefore have also been studying dioxygen reactions employing tridentate ligands with copper in combination with hemes.

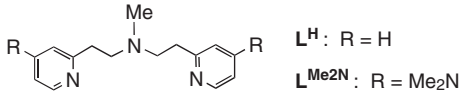

Tridentate ligands encompassing the *N*,*N*-bis[2-(2-pyridyl)-ethyl)methylamine moiety (see diagram above) are known to form copper(I) complexes with a rich dioxygen chemistry.[36–38] When the copper(I) complex with L^H, $[(L^H)Cu^I]^+$, is reacted with $(F_8)Fe^{II}$ and dioxygen, spectroscopic and stopped-flow kinetic studies provided evidence that a metastable heme–peroxo–copper complex formed; this subsequently transformed to a μ-oxo product $[(F_8)Fe^{III}–(O^{2-})–Cu^{II}(L^H)]^+$.[39] Thus, again with tridentate systems for copper, Scheme 1 is followed. Considerably more insight could be obtained with the analogue L^{Me2N}.[27] From the room temperature work-up of the heme/Cu/O_2 reaction, X-ray analysis of the corresponding μ-oxo product $[(F_8)Fe^{III}–(O^{2-})–Cu^{II}(L^{Me2N})]^+$ showed a severely bent Fe–O–Cu moiety, Figure 5.[27] This strongly contrasts with the known structure of $[(F_8)Fe^{III}–(O^{2-})–Cu^{II}(TMPA)]^+$ with tetradentate TMPA ligand, which exhibits a nearly linear Fe–O–Cu arrangement (Figure 5).[32] This was a first indication and insight showing that tridentate vs tetradentate copper chelation effects large differences in the properties of their corresponding heme–Cu assemblies.

When $[(L^{Me2N})Cu^I]^+$, $(F_8)Fe^{II}$, and O_2 are reacted in CH_2Cl_2/6% EtCN at low temperature, benchtop spectroscopic (UV–vis and NMR) monitoring revealed the presence of peroxo species $[(F_8)Fe^{III}–(O_2^{2-})–Cu^{II}(L^{Me2N})]^+$ (**3**, Figure 2), with NMR spectroscopic characteristics (i.e., pyrrole downfield and Cu-ligand upfield resonances) suggesting a high-spin $S = 2$ formulation; resonance Raman spectroscopy confirmed the presence of a peroxo moiety, two conformers exist: ν(O–O) = 767 ($\Delta^{18}O_2 = -41$) and 752 ($\Delta^{18}O_2 = -45$) cm^{-1} (Figure 2).[27] These values are strikingly lower than those for heme–peroxo–copper units with tetradentate copper ligation, suggesting a different structure is present. This will be discussed further, below.

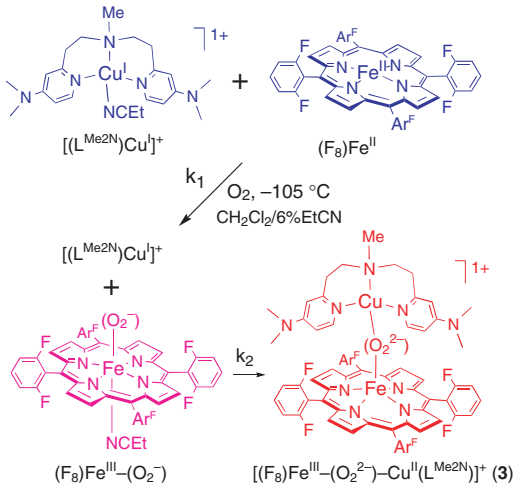

Figure 6. Dioxygen reactivity of $[(L^{Me2N})Cu^{I}]^{+}/(F_8)Fe^{II}$ 1:1 mixtures, leading to the initial formation of a heme-superoxo complex, which is attacked by the tridentate copper(I) complex, forming μ-peroxo species **3**.

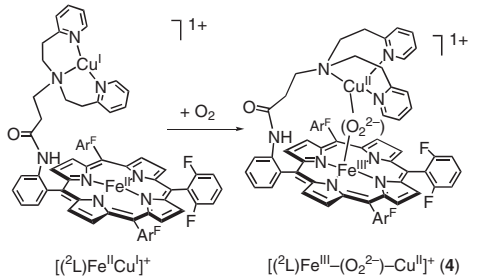

Scheme 3.

Low-temperature stopped-flow kinetics provide further insights.[27] The 1:1 $[(L^{Me2N})Cu^{I}]^{+}/(F_8)Fe^{II}/O_2$ mixture reacts very rapidly to give a heme-superoxo complex {a six-coordinate low-spin oxy-myoglobin synthetic analogue $[(EtCN)(F_8)Fe^{III}–(O_2^{-})]$ which is stable at reduced temperatures in the absence of copper complexes, $\nu(O–O) = 1178$ ($\Delta^{18}O_2 = -64$) cm^{-1}, in THF as solvent}, with $k_1 = 4 \times 10^3\ M^{-1}s^{-1}$ at $-105\,^{\circ}C$. In the solvent employed (CH_2Cl_2/6% EtCN), the nitrile present ligates strongly to the tridentate Cu(I) center, inhibiting $[(L^{Me2N})Cu^{I}]^{+}$–dioxygen reactivity. However, the $[(L^{Me2N})Cu^{I}]^{+}$ does react with the oxy-heme species, affording the μ-peroxo product $[(F_8)Fe^{III}–(O_2^{2-})–Cu^{II}(L^{Me2N})]^{+}$ (**3**), $k_2 \approx 10^5\ M^{-1}s^{-1}$ (Figure 6).

Finally, recent work further adds to the 'database' of heme–peroxo–copper compounds with tridentate copper coordination. Complex $[(^2L)Fe^{III}–(O_2^{2-})–Cu^{II}]^{+}$ (**4**)[40] (Figure 2) utilizes the L^H tridentate (see diagram above), and forms by oxygenation of the reduced precursor $[(^2L)Fe^{II}Cu^{I}]^{+}$ (Scheme 3); it is stable at low temperatures in a variety of organic solvents.[28] Resonance Raman and other spectroscopic criteria confirm the peroxo formulation, and as indicated in Figure 2, $\nu(O–O) = 747\ cm^{-1}$, the lowest value known in heme–peroxo–copper systems.

♦ *Heme–Peroxo–Copper Stuctures: End-on vs Side-on Binding*

The compounds discussed (Figure 2) represent a series of new types of O_2-adducts, those formed from $heme Fe^{II}/Cu^{I}$ dioxygen reactions.[1] The evidence suggests that there are likely major differences in structures of these heme–peroxo–copper complexes as one goes from systems with tetradentate to tridentate ligands on the copper(II) ion. There are differences in μ-oxo structures (near linear for tetradentates, bent for tridentate, Figure 5) and UV–vis features in the Q-band region.[28] As outlined in some detail, there are dramatic variations in the peroxo $\nu(O–O)$ stretching frequencies, i.e., with much lower values for the tridentate containing systems (Figure 2). Changes in geometries and resulting bond angles are known to result in large variations in $\nu(O–O)$ values for non-heme peroxo-diferric species.[41]

We present here further arguments in favor of a major changes in peroxo ligation and suggestions for proposed structures for the complexes **1**–**4**. In peroxo–dicopper(II) complexes, it is now established that ligands have a profound influence on copper-dioxygen chemistry.[5] With tetradentate ligands, end-on μ-1,2-peroxo ligation is preferred, but with tridentate chelates, side-on μ-η^2:η^2-peroxo coordination is most common (Figure 7A).[5] Strikingly, the peroxo vibrational properties for the latter side-on complexes are quite different, with very low ($<760\ cm^{-1}$) $\nu(O–O)$ values observed (Figure 7A), ascribed to back-bonding from copper to the peroxo antibonding σ^* orbital which considerably weakens the O–O bond.[5,42,43] As already described, $[(TMP)Fe^{III}–(O_2^{2-})–(5MeTPA)Cu^{II}]^{+}$ (**2***) (Figure 4) possesses $\nu(O–O) = 790\ cm^{-1}$,[26] and a series of high-spin heme–Fe^{III} peroxo complexes $[(P)Fe^{III}(O_2^{2-})]^{-}$ from Valentine and co-workers show $\nu(O–O)$ stretching frequencies very close to $800\ cm^{-1}$ (Figure 7A).[44] In order to achieve a lowering of

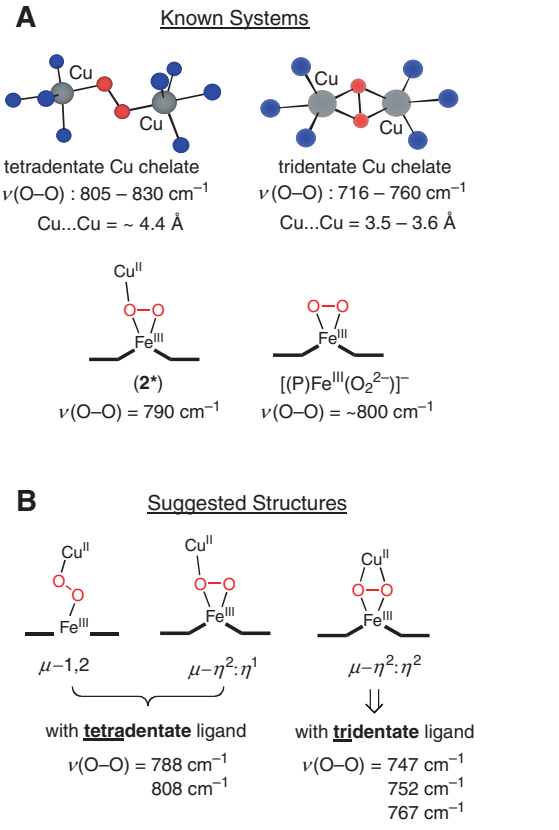

Figure 7. Structures and Properties of known peroxo–dicopper, heme–peroxo–copper, and peroxo–heme complexes (**A**), and structures proposed for heme–peroxo–complexes discussed in this paper (**B**).

the O–O stretching frequency from the 800 cm^{-1} region (for **2**** or $[(P)Fe^{III}(O_2^{2-})]^-$) to near 750 cm^{-1} as seen in **3** and **4**, we conclude that these complexes therefore possess side-on μ-η^2:η^2-peroxo heme–copper coordination, Figure 7B, consistent with the coordination tendencies known for copper(II) ion with tridentate chelates. For complexes **1** and **2** containing copper tetradentates and which have an overall complex architecture similar to that in the Naruta compound **2****, μ-η^2:η^1-peroxo heme–copper ligation also seems likely, although the possibility of μ-1,2-peroxo ligation (Figure 7B) cannot be ruled out.

♦ Summary and Future Directions

The O_2 binding and reductive O–O cleavage chemistry occurring in heme–copper oxidases has inspired recent efforts to probe basic aspects of dioxygen chemistry with synthetic heme–copper assemblies. Some of these studies, especially those emphasizing the isolation and characterization of discrete heme–copper O_2-adducts, have been described here. The focus has been on comparing and contrasting chemistry with tetradentate vs tridentate copper chelation. As described, profound structural effects are observed, and tridentate Cu-ligation dramatically weakens the O–O bond in heme–peroxo–copper complexes, as seen by the greater than 50 cm^{-1} lowering of the O–O stretching frequency. Confirmation or elucidation of structures needs to be carried out, and correlation of structure with spectroscopic and chemical properties will be important in future investigations.

The present studies provide us new fundamental insights into metal dioxygen chemistry. As mentioned in earlier remarks, these heme–copper dioxygen adducts (i.e., **1**–**4**) are not necessarily models for discrete heme–copper oxidase turnover intermediates, since they have smaller Fe···Cu distances than can probably exist in the enzymes, and no strong axial-base ligand (e.g., an imidazole) is present. Further, they do not possess an imidazole–phenol moiety ligated to copper, mimicking the His–Tyr crosslink found in the enzyme active sites; progress in the development of model systems with imidazole–phenol moieties is occurring.[1,45–47] However, the ability to generate complexes such as **1**–**4** now places researchers in the position to investigate or model aspects of the enzyme O–O cleavage process. Complexes **1**–**4**, with either μ-1,2-, μ-η^2:η^1- or μ-η^2:η^2-peroxo heme–Cu structures, can in the near future be studied in reactions with proton/electron sources, and/or with imidazole or pyridine moieties as models for an enzyme heme a_3 proximal histidine group. Does addition of such a 'base' effect heme–peroxo–copper complex (**1**–**4**) high-spin to low-spin conversion and/or does it change the peroxo bridging structure? Does addition of H^+/e^- lead to O–O cleavage and production of an oxo–ferryl Fe^{IV}=O moiety and Cu^{II}–hydroxide, as probably occurs in the enzyme (Figure 1)? Is the 'base' also required for the latter to occur? Exciting times lie ahead for the study of new heme–copper O_2-chemistry.

References

1 E. Kim, E. E. Chufan, K. Kamaraj, and K. D. Karlin, *Chem. Rev.*, **104**, 1077 (2004).
2 K. D. Karlin, *Science*, **261**, 701 (1993).
3 J. P. Collman, R. Boulatov, C. J. Sunderland, and L. Fu, *Chem. Rev.*, **104**, 561 (2004).
4 M. Momenteau and C. A. Reed, *Chem. Rev.*, **94**, 659 (1994).
5 L. M. Mirica, X. Ottenwaelder, and T. D. P. Stack, *Chem. Rev.*, **104**, 1013 (2004).
6 E. A. Lewis and W. B. Tolman, *Chem. Rev.*, **104**, 1047 (2004).
7 L. Que, Jr. and W. B. Tolman, *Angew. Chem., Int. Ed.*, **41**, 1114 (2002).
8 C. X. Zhang, H.-C. Liang, K. J. Humphreys, and K. D. Karlin, in "Catalytic Activation of Dioxygen by Metal Complexes," ed. by L. Simandi, Kluwer, Dordrecht, The Netherlands (2003), Chap. 2, pp 79–121.
9 S. Ferguson-Miller and G. T. Babcock, *Chem. Rev.*, **96**, 2889 (1996).
10 H. Michel, J. Behr, A. Harrenga, and A. Kannt, *Annu. Rev. Biophys. Biomol. Struct.*, **27**, 329 (1998).
11 S. Yoshikawa, K. Shinzawa-Itoh, R. Nakashima, R. Yaono, E. Yamashita, N. Inoue, M. Yao, M. J. Fei, C. P. Libeu, T. Mizushima, H. Yamaguchi, T. Tomizaki, and T. Tsukihara, *Science*, **280**, 1723 (1998).
12 C. Ostermeier, A. Harrenga, U. Ermler, and H. Michel, *Proc. Natl. Acad. Sci. U.S.A.*, **94**, 10547 (1997).
13 M. Svensson-Ek, J. Abramson, G. Larsson, S. Tornroth, P. Brzezinski, and S. Iwata, *J. Mol. Biol.*, **321**, 329 (2002).
14 T. Soulimane, G. Buse, G. P. Bourenkov, H. D. Bartunik, R. Huber, and M. E. Than, *EMBO J.*, **19**, 1766 (2000).
15 J. Abramson, *et al.*, *Nat. Struct. Biol.*, **7**, 910 (2000).
16 T. Tsukihara, H. Aoyama, E. Yamashita, T. Tomizaki, H. Yamaguchi, K. Shinzawa-Itoh, R. Nakashima, R. Yaono, and S. Yoshikawa, *Science*, **269**, 1069 (1995).
17 S. Iwata, C. Ostermeier, B. Ludwig, and H. Michel, *Nature*, **376**, 660 (1995).
18 A. Harrenga and H. Michel, *J. Biol. Chem.*, **274**, 33296 (1999).
19 M. R. Cheesman, V. S. Oganesyan, N. J. Watmough, C. S. Butler, and A. J. Thomson, *J. Am. Chem. Soc.*, **126**, 4157 (2004).
20 H. C. Fry, D. V. Scaltrito, K. D. Karlin, and G. J. Meyer, *J. Am. Chem. Soc.*, **125**, 11866 (2003).
21 M. R. A. Blomberg, P. E. M. Siegbahn, and M. Wikström, *Inorg. Chem.*, **42**, 5231 (2003).
22 J. P. Collman, R. Boulatov, and C. J. Sunderland, *Porphyrin Handbook*, **11**, 1 (2003).
23 A. Didier, M. L'Her, and B. Boitrel, *Org. Biomol. Chem.*, **1**, 1274 (2003).
24 R. A. Ghiladi, K. R. Hatwell, K. D. Karlin, H.-w. Huang, P. Moënne-Loccoz, C. Krebs, B. H. Huynh, L. A. Marzilli, R. J. Cotter, S. Kaderli, and A. D. Zuberbühler, *J. Am. Chem. Soc.*, **123**, 6183 (2001).
25 R. A. Ghiladi, T. D. Ju, D.-H. Lee, P. Moënne-Loccoz, S. Kaderli, Y.-M. Neuhold, A. D. Zuberbühler, A. S. Woods, R. J. Cotter, and K. D. Karlin, *J. Am. Chem. Soc.*, **121**, 9885 (1999).
26 T. Chishiro, Y. Shimazaki, F. Tani, Y. Tachi, Y. Naruta, S. Karasawa, S. Hayami, and Y. Maeda, *Angew. Chem., Int. Ed.*, **42**, 2788 (2003).
27 E. Kim, M. E. Helton, I. M. Wasser, K. D. Karlin, S. Lu, H.-w. Huang, P. Moënne-Loccoz, C. D. Incarvito, A. L. Rheingold, M. Honecker, S. Kaderli, and A. D. Zuberbühler, *Proc. Natl. Acad. Sci. U.S.A.*, **100**, 3623 (2003).
28 E. Kim, J. Shearer, S. Lu, P. Moenne-Loccoz, M. E. Helton, S. Kaderli, A. D. Zuberbuhler, and K. D. Karlin, *J. Am. Chem. Soc.*, in press.
29 K. D. Karlin, S. Kaderli, and A. D. Zuberbühler, *Acc. Chem. Res.*, **30**, 139 (1997).
30 K. D. Karlin and A. D. Zuberbühler, in "Bioinorganic Catalysis: Second Edition, Revised and Expanded," ed. by J. Reedijk, E. Bouwman, Marcel Dekker, Inc., New York (1999), pp 469–534.
31 A. Nanthakumar, S. Fox, N. N. Murthy, and K. D. Karlin, *J. Am. Chem. Soc.*, **119**, 3898 (1997).
32 K. D. Karlin, A. Nanthakumar, S. Fox, N. N. Murthy, N. Ravi, B. H. Huynh, R. D. Orosz, and E. P. Day, *J. Am. Chem. Soc.*, **116**, 4753 (1994).
33 T. D. Ju, R. A. Ghiladi, D.-H. Lee, G. P. F. van Strijdonck, A. S. Woods, R. J. Cotter, V. G. Young, Jr., and K. D. Karlin, *Inorg. Chem.*, **38**, 2244 (1999).
34 H. V. Obias, G. P. F. van Strijdonck, D.-H. Lee, M. Ralle, N. J. Blackburn, and K. D. Karlin, *J. Am. Chem. Soc.*, **120**, 9696 (1998).
35 Y. Naruta, T. Sasaki, F. Tani, Y. Tachi, N. Kawato, and N. Nakamura, *J. Inorg. Biochem.*, **83**, 239 (2001).
36 H. V. Obias, Y. Lin, N. N. Murthy, E. Pidcock, E. I. Solomon, M. Ralle, N. J. Blackburn, Y.-M. Neuhold, A. D. Zuberbühler, and K. D. Karlin, *J. Am. Chem. Soc.*, **120**, 12960 (1998).
37 E. Pidcock, S. DeBeer, H. V. Obias, B. Hedman, K. O. Hodgson, K. D. Karlin, and E. I. Solomon, *J. Am. Chem. Soc.*, **121**, 1870 (1999).
38 C. X. Zhang, H.-C. Liang, E. Kim, J. Shearer, M. E. Helton, E. Kim, S. Kaderli, C. D. Incarvito, A. D. Zuberbühler, A. L. Rheingold, and K. D. Karlin, *J. Am. Chem. Soc.*, **125**, 634 (2003).
39 M. A. Kopf, Y. M. Neuhold, A. D. Zuberbühler, and K. D. Karlin, *Inorg. Chem.*, **38**, 3093 (1999).
40 K. D. Karlin, E. Kim, R. A. Ghiladi, M. E. Helton, J. Shearer, S. Lu, H. Huang, and P. Moenne-Loccoz, *J. Inorg. Biochem.*, **96**, 163 (2003).
41 T. C. Brunold, N. Tamura, N. Kitajima, Y. Moro-Oka, and E. I. Solomon, *J. Am. Chem. Soc.*, **120**, 5674 (1998).
42 a) P. K. Ross and E. I. Solomon, *J. Am. Chem. Soc.*, **113**, 3246 (1991). b) P. K. Ross and E. I. Solomon, *J. Am. Chem. Soc.*, **112**, 5871 (1990).
43 E. I. Solomon, F. Tuczek, D. E. Root, and C. A. Brown, *Chem. Rev.*, **94**, 827 (1994).
44 M. Selke, M. F. Sisemore, and J. S. Valentine, *J. Am. Chem. Soc.*, **118**, 2008 (1996).
45 K. Kamaraj, E. Kim, B. Galliker, L. N. Zakharov, A. L. Rheingold, A. D. Zuberbuehler, and K. D. Karlin, *J. Am. Chem. Soc.*, **125**, 6028 (2003).
46 J. G. Liu, Y. Naruta, F. Tani, T. Chishiro, and Y. Tachi, *Chem. Commun.*, **2004**, 120.
47 J. P. Collman, R. A. Decreau, and S. Costanzo, *Org. Lett.*, **6**, 1033 (2004).